Evaluation of the Kinetic Parameters

We begin with the Butler-Volmer equation to represent the ferri-ferrocyanide system

$$i = i_o \left[\left(\frac{i_{l,a} - i}{i_{l,a}} \right) \exp\left[\frac{\alpha n \mathbf{F}}{RT} \eta \right] - \left(\frac{i_{l,c} - i}{i_{l,c}} \right) \exp\left[\frac{-(1-\alpha) n \mathbf{F}}{RT} \eta \right] \right] \quad [A\text{-}2]$$

where i_o is the exchange current density, α is the transfer coefficient, and $i_{l,a}$ and $i_{l,c}$ are the anodic and cathodic limiting current densities. By differentiating i w.r.t.η and evaluating the result at $\eta = 0$, we obtain

$$i_o = \frac{\left(\frac{di}{d\eta} \right)_{\eta=0}}{\frac{n\mathbf{F}}{RT} + \left(\frac{1}{i_{l,c}} - \frac{1}{i_{l,a}} \right) \left(\frac{di}{d\eta} \right)_{\eta=0}} \quad [A\text{-}3]$$

This equation allows one to evaluate i_o from experimental data at each rotating speed. The average value of i_o over the six rotation speeds was found to be 5.73 mA/cm^2. The transfer coefficient α can then be evaluated by applying Eq. [A-1] to the experimental data. The value of α was estimated to be 0.16.

For a system with an excess supporting electrolyte, η is the sum of η_c and η_a where η_a is the activation overpotential which can be determined by

$$i = i_o \left[\exp\left(\frac{\alpha n \mathbf{F}}{RT} \eta_a \right) - \exp\left(\frac{-(1-\alpha) n \mathbf{F}}{RT} \eta_a \right) \right] \quad [A\text{-}4]$$

η_c can now be determined by subtracting η_a from η which has been determined experimentally.

LIST OF SYMBOLS

a	a constant defined in Eq. [6]
c_b, c_i	concentration of reacting ion at the electrode surface and in the bulk solution, respectively
D	diffusion coefficient of reacting ion
$\mathbf{F}$	Faraday's constant
i	current density
i_{dc}, i_p	d-c current density, and pulsed current density, respectively
$(i_{dc})_l$	d-c limiting current density
$i_{l,a}$, $i_{l,c}$	anodic limiting current density and cathodic limiting current density, respectively
i_o	exchange current density
n	number of electrons transferred in reaction
N	number of cycles in a pulse train
R	universal gas constant
Sc	Schmidt number
T	temperature
t	time
α	transfer coefficient
δ	thickness of the Nernst diffusion layer
η	overpotential
η_a, η_c	activation overpotential and pulse concentration, respectively
$(\eta_{dc})_c$, $(\eta_p)_c$	d-c concentration overpotential and pulse concentration overpotential, respectively
θ_1, θ_2, θ	on-time, off-time, and cycle time of a pulse, respectively
ν	kinematic viscosity of the electrolyte
τ	time defined in Eq. [7]
ω	rotation speed

REFERENCES

1. H. Y. Cheh, *This Journal*, **118**, 551 (1971).
2. N. Ibl, *Surf. Technol.*, **10**, 81 (1980).
3. J. M. Hale, *J. Electroanal. Chem. Interfacial Electrochem.*, **6**, 187 (1963).
4. J. M. Hale, *ibid.*, **8**, 332 (1964).
5. K. Viswanathan, M. A. F. Epstein, and H. Y. Cheh, *This Journal*, **125**, 1772 (1978).
6. J. Newman, "Electrochemical Systems," Prentice-Hall, Englewood Cliffs, NJ (1973).
7. J. Newman, in "Advances in Electrochemistry and Electrochemical Engineering," Vol. 5, P. Delahay and C. W. Tobias, Editors, p. 87, Interscience Publishers, New York (1967).

Investigation of Laser-Enhanced Electroplating Mechanisms

J. Cl. Puippe,*[1] R. E. Acosta,* and R. J. von Gutfeld

IBM Thomas J. Watson Research Center, Yorktown Heights, New York 10598

ABSTRACT

The mechanism responsible for the very high plating rates at electrodes illuminated by a laser beam was investigated. Absorption of the laser energy by the electrode results in a localized increase in temperature at the metal-solution interface. This leads to: (*i*) a shift in the rest potential, (*ii*) an increase in the charge transfer rate, and (*iii*) strong microstirring of the solution due to thermal gradients and, at high laser power densities, to strong local boiling. Verification of the first two effects was achieved by measuring the enhancement in plating rates as a function of overpotential, laser power, and substrate thickness and by comparing these results with measurements using solutions at various bulk temperatures. Observation of the cathode through a video monitor, as well as detection of bubble formation using a miniature microphone, verified that a correlation exists between the ejection of bubbles from the cathode and sharp increases in the current. Application of laser-enhanced electroplating for maskless generation of patterns is also briefly discussed.

A large local increase of current density at the point of incidence of a laser beam on a cathode was first reported by von Gutfeld *et al.* (1-3). Plating rates enhanced by as much as a factor of 1000 were reported for nickel, copper, and gold deposition. It has been shown (2-4) that electroless plating and electroetching rates can also be substantially increased by absorption of laser light.

In this paper a study of the enhancement mechanism is presented. The aim was to investigate whether the laser enhancement is due only to strong microstirring of the solution or whether it is due to a significant increase in the charge transfer rate. In other words, if the reaction were not mass transport limited, would the reaction rate be influenced significantly by the

* Electrochemical Society Active Member.
[1] Present address: Werner Flühmann AG, Ringstrasse 9, 8600 Dubendorf, Switzerland.

Key words: battery, boiling, masking, mass transport.

laser light absorption? In order to answer this question the laser-enhanced plating rates were measured as a function of overpotential.

Previous experiments showed that back illumination of a thin cathode led to the same enhancement as that for front illumination (1). Hence a significant contribution of a photocatalytic effect is excluded. We therefore postulate that the phenomena involved are related to a local increase of temperature at the metal-solution interface as a result of laser light absorption. The findings reported in this paper permit us to elaborate on a thermal model for the explanation of the observed plating current enhancements. The influence of the laser power and the substrate thickness (which influences the radial heat flow in the cathode) on the deposition rate and on the plated spot diameter were also investigated.

Fundamental Studies

Experimental conditions.—Experiments were conducted under potentiostatic control in a Pyrex glass cell containing vertical electrodes approximately 1 cm on a side, Fig. 1. The laser light was directed normally onto the cathode through a small hole in the anode. The anode consisted of a copper plate, the cathode of a thin film of gold or copper. Thin films were used to reduce heat dissipation in the cathode. In some experiments a small, well-defined, active area was required. The cathode was then covered by a photoresist layer a few microns thick, except for a hole of the same diameter as the laser beam, measured to $\sim 1/e$ of its maximum intensity. The details of this structure are given in Fig. 2. The laser beam diameter was adjusted by positioning a microscope objective lens (2.5×) at a distance from the sample so that 67% of the laser power was incident on the active area of the cathode. The laser wavelength was chosen so that the laser beam was essentially not absorbed in the electrolyte, but was at least partially absorbed at the cathode. The experimental conditions are summarized in Table I.

Enhanced plating rates as a function of overpotential.—Figure 3 shows the polarization curve for the system $Cu/CuSO_4$ without laser irradiation. In this curve one clearly distinguishes the overpotential region in which the current is mass transport limited from the region where charge transfer is the limiting step of the reaction. Figure 4 shows the polarization curve of the same system with periodic irradiation by the laser. Here the laser beam diameter was equal to

Table I. Experimental conditions

Solution	$CuSO_4$, 0.05M H_2SO_4, 1M
Electrode	Metallic film: Au or Cu Metallic film thickness: 500-10,000Å
Laser	Beam diameter: 100-500 μm Incident laser power density: 0.1-2 kW/cm² Wavelength: 5145Å

that of the active cathode area (*i.e.*, 200 μm). Periodic pulsing of the laser was used to prevent excessive plating buildup that would result from continuous irradiation. This ensures a more accurate measurement of the plating enhancement, since the cathode is little changed during the short duration of the laser pulses. Figure 5 shows the same polarization curve as Fig. 4, but with a logarithmic current scale. The logarithmic current scale allows a more accurate reading of the current enhancement. The apparent slower current response is due to an artifact of the apparatus. The different overvoltage regions of the comb-shaped curves (Fig. 4 and 5) are analyzed in more detail below.

The mass transport controlled region.—According to the limiting current plateau of the polarization curve of Fig. 3, the mass transport controlled deposition extends from an overpotential of −200 to −650 mV. In

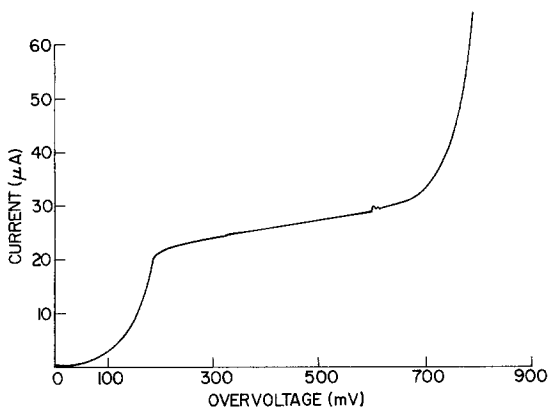

Fig. 3. Polarization curve for copper electrodeposition at room temperature with the cathode of Fig. 2 (current and overvoltage are negative). Electrode diameter, 550 μm; voltage scanning speed, 4 mV/sec.

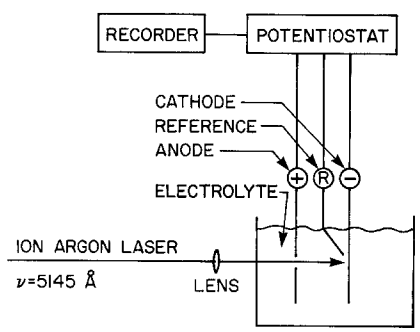

Fig. 1. Schematic of the apparatus

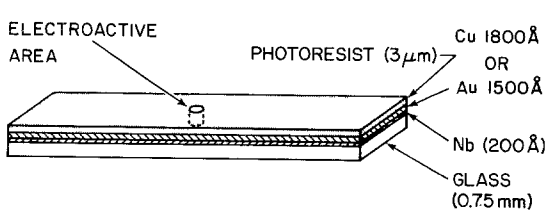

Fig. 2. Structure of the cathode and typical thicknesses of the various layers.

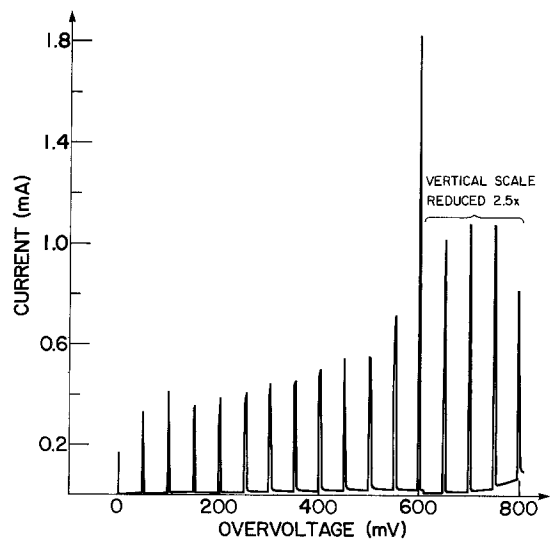

Fig. 4. Polarization curve for copper electrodeposition with periodic laser illumination (cathode of Fig. 2). Laser power, 210 mW; electrode diameter = laser beam diameter = 200 μm; voltage scanning speed, 5 mV/sec.

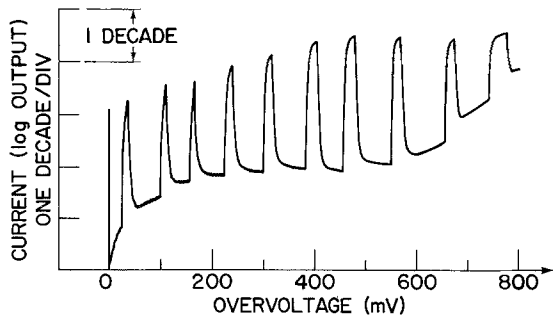

Fig. 5. Polarization curve for copper electrodeposition with periodic laser illumination on cathode of Fig. 2 (log current scale). Incident laser power, 500 mW; electrode diameter, 200 μm; voltage scanning speed, 5 mV/sec.

this region the maximum enhancement[2] measured on an electrode of the same size as the laser beam is 400×, Fig. 5. A current density of more than 18 A/cm^2 is reached. This plating rate, which is extremely high for this dilute solution, corresponds to a deposit growth rate of more than 6 μm/sec. Other experiments in the mass transport controlled region, with the electrode not defined by a hole in the photoresist but rather on a plain wafer of 1 cm^2 area, resulted in enhanced plating rates of more than 1000×, like those reported earlier (1). The apparent discrepancy is due to a smaller limiting current density without laser for large area electrodes. A decrease in the electrode size to very small dimensions leads to diffusion which is no longer one dimensional but spherical, and thereby increases the value of the limiting current for these small area cathodes. The influence of the electrode diameter on the limiting current density is shown in Fig. 6. The enhancement ratio for an electrode with an area much larger than the cross section of the laser beam is determined taking into account the small area irradiated by the laser. However, the enhancement is referred to the limiting current density of the large electrode, thus such cathodes show enhancements three times larger than the values shown in Fig. 4 and 5.

We attribute the enhancement of the limiting current to stirring through local convection of the solution due to a strong thermal gradient near the cathode interface (1, 2). We have also found that for higher laser power densities local boiling of the solution produces strong additional stirring. Observation of the cathode through a video monitor showed that the bubbles were ejected into the solution normally from the vertical electrode. The effect of this additional stirring has been measured quantitatively by recording the limiting current density for the copper deposition while the cathode was illuminated by pulsed laser light, the intensity of which produced boiling of the solution at the cathode. The bubble formation generated an acoustic wave which was detected with a miniature microphone attached to the external wall of the cell. Figure 7 shows both the acoustic wave (trace A) and the limiting current (trace B) simultaneously recorded on a dual beam oscilloscope. Six milliseconds after the beginning of the light pulse, trace A showed a sharp increase in the acoustic signal due to boiling of the solution, and at the very same time the limiting current increased by a factor of 4. This increase in the limiting current is due to the stirring generated by the ejection of one or more bubbles in the solution.

[2] The enhancement is the ratio of the plating current obtained with and without laser illumination.

The charge transfer controlled region.—The comb-shaped curves of Fig. 4 and 5 also show significant increases in the current for overpotentials well below the region where the reaction is mass transport limited. The increase in the reaction rate is believed to be due to higher temperature produced in the region of laser light absorption. The influence of temperature on the reaction rate has been studied quantitatively in a separate experiment in which the entire volume of the electrolyte was heated. The results are shown in Fig. 8. At a potential of −20 mV an increase of temperature from 25° to 85°C speeds up the reaction by a factor of more than 50.

It is seen from the curves of Fig. 8 that a shift of rest potential toward more positive values occurs with increasing temperature. This shift in rest potential is shown in more detail in Fig. 9. A shift of the equilibrium potential with increasing temperature is expected from thermodynamic considerations (5). The shift of the rest potential has been measured as a function of the laser power (Fig. 10) on an electrode of the same diameter as the laser beam. By comparing the results of Fig. 9 and 10 one obtains a relationship between the incident laser power density and the temperature at the interface, Fig. 11. The domain of extrapolation (B-C) gives approximate values for the interfacial temperature as a function of incident laser power density. A separate experiment showed that for laser power densities between B and C, strong boiling occurred with bubbles ejected normally from the cathode. This is consistent with the temperatures obtained by extrapolation.

Due to the positive shift of the rest potential at the hotter part of the cathode it is possible to plate locally on a large electrode with no background plating. This is achieved by maintaining the cathode at the potential value corresponding to the rest potential of the

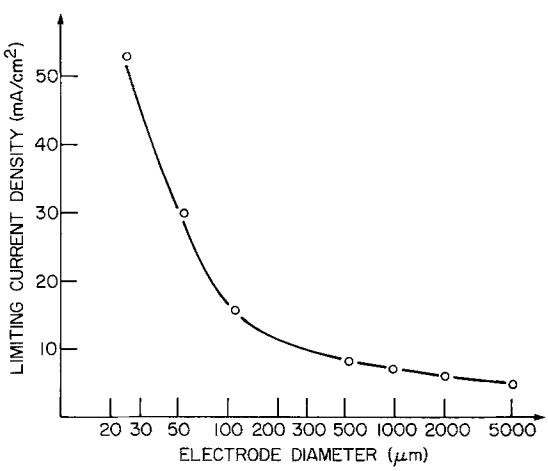

Fig. 6. Influence of the electrode diameter on the limiting current density of copper deposition without laser irradiation.

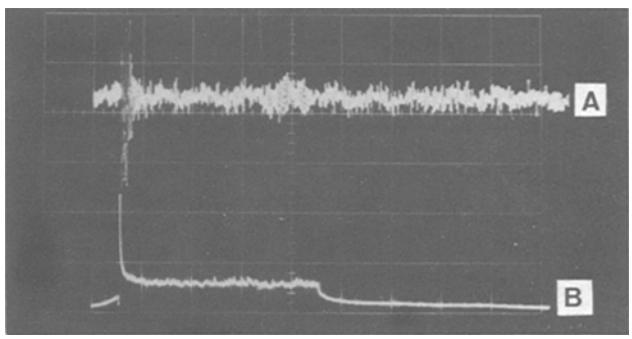

Fig. 7. The influence of boiling on the stirring of the solution. Trace A: acoustic signal; trace B: limiting current density for the system described in Table I. Abscissa, 10 msec/div for A and B; ordinate, 2 mA/div for B. Substrate: see Fig. 2, with Cu 1800Å, no photoresist. Laser pulse length, 45 msec; duty cycle, 1/4; incident laser power during the on time, 320 mW. Laser beam diameter, approximately 200 μm.

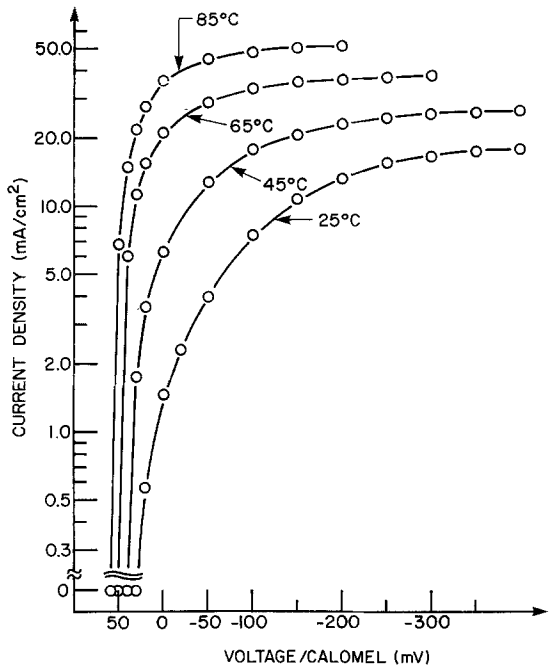

Fig. 8. Influence of temperature on the polarization curves of $Cu/CuSO_4$. A rotating disk electrode (200 rpm) with a diameter of 7.6 mm was used.

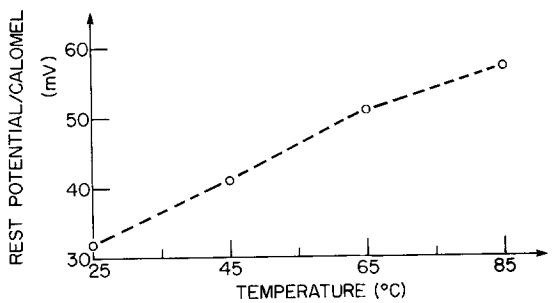

Fig. 9. Rest potential of the system $Cu/CuSO_4$ as a function of electrolyte temperature.

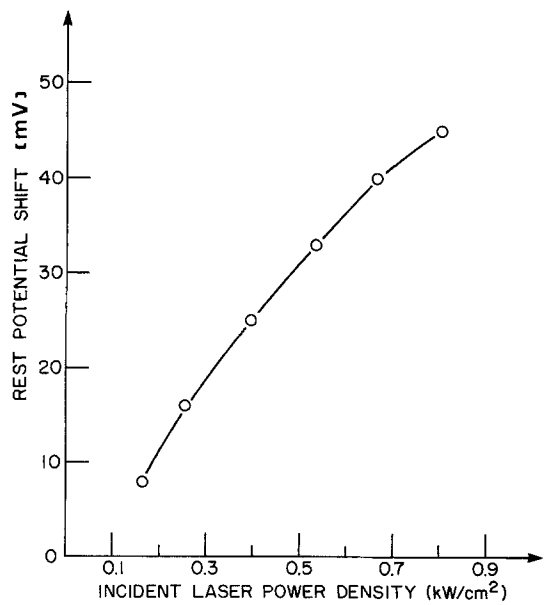

Fig. 10. Rest potential shift for the system $Cu/CuSO_4$ as a function of laser power density.

system Cu/Cu^{++} at room temperature. Since the illuminated part then has a more positive rest potential than the potential imposed on the rest of the elec-

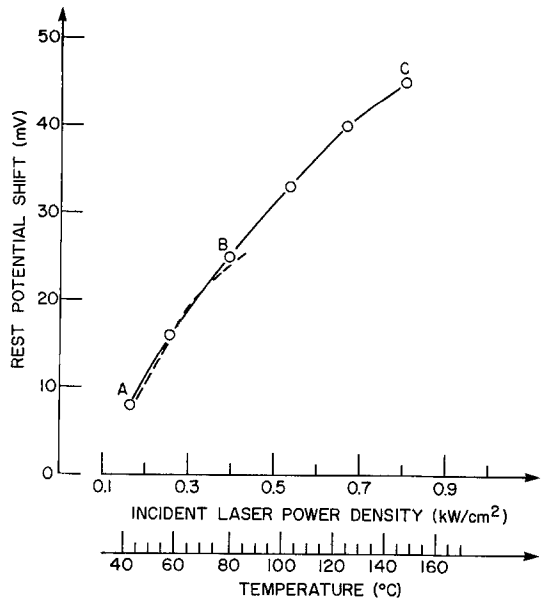

Fig. 11. Rest potential shift as a function of laser power density, indicated by ———, and of temperature indicated by - - - -. The figure is a superposition of Fig. 9 and 10. A, B, and C are referred to in the text.

trode, plating occurs there and only there. According to the definition of enhancement previously given, the enhancement approaches infinity; however the absolute current increase is found to be one order of magnitude lower than under mass transport controlled conditions. Figure 12 shows the current densities obtained at different overpotentials as a function of the laser power density. The curve at $\eta = 0$ corresponds to the conditions for no background plating; the curve at $\eta = -50$ mV is in the charge transfer controlled region, and the one at $\eta = -600$ mV is in the mass transport controlled region.

The shift of the rest potential has other implications. The situation in which two regions of different rest potentials are electrically connected constitutes a battery. Thus, laser light focused onto a copper electrode immersed in an electrolyte will result in simul-

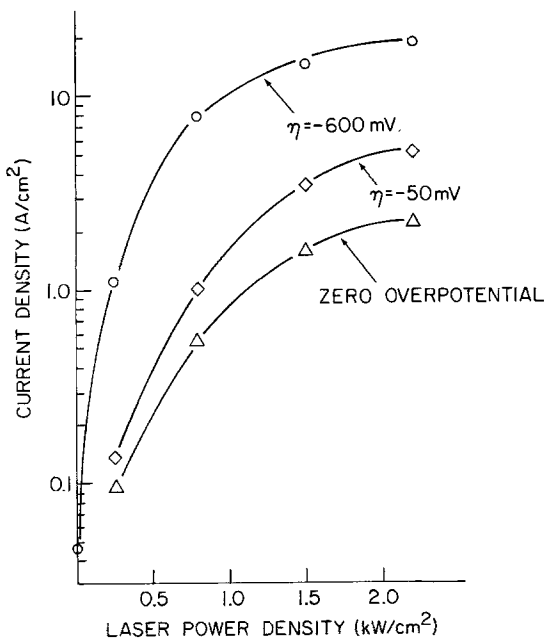

Fig. 12. Laser-enhanced current densities for different overpotentials as a function of the laser power density. Base: Nb, 200 Å/1500Å evaporated on glass; electrode diameter, 200 μm; overpotential values referred to room temperature.

taneous plating and etching without the use of an electrical circuit. For the solution in Table I, plating occurs in the region of higher temperature, *i.e.*, the region of laser light absorption, while simultaneous etching occurs in the colder adjacent regions. For a circular beam, this will result in a plated central circular spot surrounded by an etched annulus, Fig. 13. The necessary condition for plating in the hotter region is a positive shift of the rest potential with increasing temperature, which is not a universal behavior for electrochemical systems. The temperature coefficient for the potential shift is determined by the negative of the entropy change for the cell reaction (5). Reference (5) gives the temperature coefficient of the equilibrium potential for several systems, both positive and negative shifts are tabulated. The system nickel/nickel citrate has been studied in our laboratory (6). It has a negative rest potential shift with increasing temperature. According to this, we expect dissolution to occur at the hotter region and plating on the adjacent colder annulus. This is shown in Fig. 14

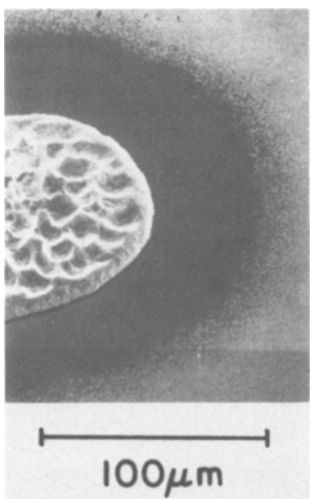

Fig. 13. SEM micrograph of copper deposited with no external electrical circuit. Base Nb, 200 Å/Cu, 1800Å evaporated on glass; incident laser power, 450 mW.

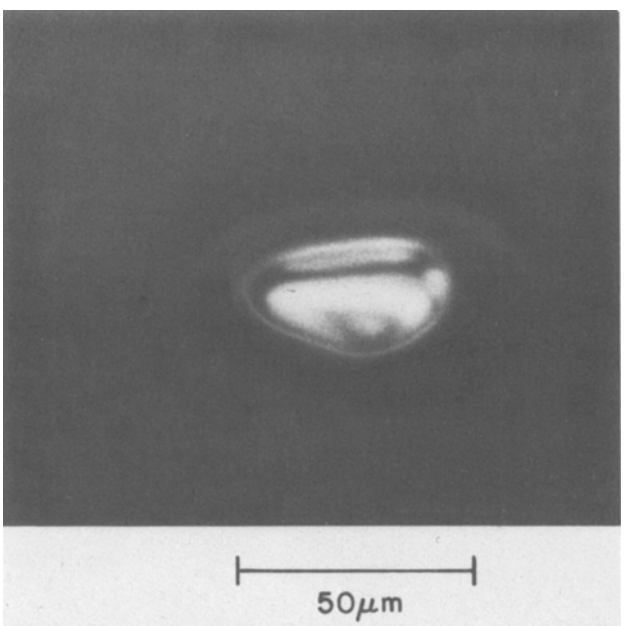

Fig. 14. SEM micrograph of nickel etching and plating with no external electrical circuit. Solution: $NiSO_4$, 0.2M; $Na_3cit.$, 0.1M; pH, 6.5. Base: Ni, 5000Å on glass; incident laser power, 650 mW.

for a nickel cathode immersed in nickel citrate solution in conjunction with a focused laser beam.

Laser-enhanced plating mechanism: thermal model. —From the considerations above we postulate that in the presence of laser light the enhancement of the reaction rate is due to an increase of temperature at the metal-solution interface, which has three separate effects: (*i*) strong microstirring of the solution due to thermal gradients, with additional stirring at high laser power densities due to strong local boiling of the solution; (*ii*) an increase in the charge transfer rate with increasing temperature. This effect is more dependent on the nature of the system metal/electrolyte than the microstirring of the solution. For aqueous plating solutions the stirring will not vary substantially from one system to another, but the variation of the reaction rate with temperature at the interface is strongly dependent on the system; and (*iii*) a shift in the rest potential. The direction and magnitude of the shift depends on the system used.

Since the temperature change at the interface is responsible for the enhancement of the reaction, several experiments were undertaken in which the temperature at the interface could be varied. This was achieved by changing either the thickness of the metallic layer of the cathode or the incident laser power density. For these experiments the electrode was maintained at the rest potential and the resulting plating in the illuminated region occurred well below the limiting current. The total charge, Q, for each deposit was equal to 5×10^{-4}C. The laser was applied for sufficiently long time intervals to insure steady-state thermal conditions at the interface. The laser beam diameter was approximately 200 μm; the thickness of the metallic film of the cathode (on a glass substrate) was varied between 500 and 10,000Å. The main effect of increasing the metallic layer thickness is a decrease in the maximum temperature attained by the cathode interface due to the increased radial heat flow. The radial heat dissipation occurs mainly in the metallic layer because of its much higher heat conductivity compared to that of the supporting glass substrate. For thick metallic layers we expect a larger plated spot diameter. This trend is observed in Fig. 15. The increase of spot diameter for substrate thicknesses ranging from 500 to 10,000Å varies by a factor of 2. The temperature along the radial direction decreases rapidly with increasing distance from the center for values greater than the beam radius, so that plating does not extend much beyond the beam circumference even with the thickest layers investigated here. Figure 15 also shows that an increase of the metallic film thickness decreases the laser enhanced current. We attribute this directly to the lower interfacial temperature.

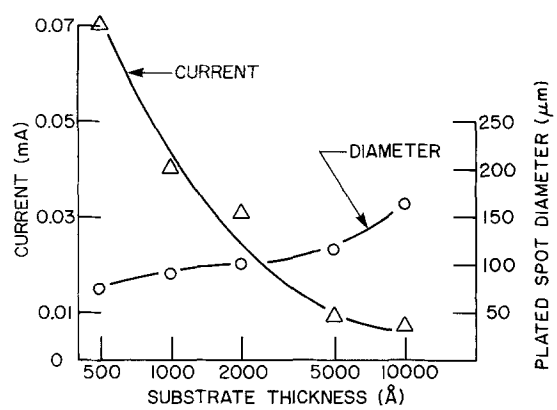

Fig. 15. Influence of the metallic film thickness on deposition rate and resulting deposited spot diameter. $Q = 5 \cdot 10^{-4}$C for each deposit; incident laser power, 100 mW.

With increasing laser power (maintaining fixed beam diameter) we observed the expected trends for the enhanced current and plated spot diameter, Fig. 16. For an incident laser power ranging from 100 to 300 mW the laser enhanced current increases by a factor of 13, whereas for the same power range the plated spot diameter increases by a factor of 2. This can again be explained by the strongly nonlinear radial temperature profile in conjunction with a sublinear plating enhancement that occurs for small temperature increases above ambient (2).

Applications

Copper lines in microcircuits have been connected or bridged using the laser-enhanced electroplating method, Fig. 17. The bridges were made by manual translation of a horizontal cathode under a focused laser beam. A lens with a magnification factor of 20 was used. The bridging work was done at low overpotential conditions which resulted in almost no background plating. The electrical resistance of these laser plated bridges is low. The solution used for this circuit repair experiment was $CuSO_4$, 0.5M/H_2SO_4, 0.01M.

Improvements in the optics used to focus the beam made it possible to reduce the width of the plated line to 2 μm. Figure 18 shows a line plated on an electrode using a copper fluoborate solution under thermobattery conditions, *i.e.*, without an external power source. This width is consistent with the limitations expected from both diffraction theory and from the aberration produced by the electrolyte layer. However, we believe this width is not the lowest attainable size. One can expect a smaller width with the use of a more elaborate lens design and possibly by decreasing the dwell time of the laser on the cathode.

For practical applications we see at least two important reasons for plating in the low overpotential region: (*i*) the possibility of avoiding, or minimizing, background plating and (*ii*) a better quality of deposit than that obtained in the mass transport controlled region.

Besides offering a means for maskless pattern generation through the use of a scannable laser beam, this technique can also result in a major cost saving when precious metals are to be deposited selectively. Clearly the technique is most useful for localized, small area plating.

Acknowledgments

We are grateful for expert technical assistance by D. R. Vigliotti throughout the experimental phase of this work. In addition we thank C. Aliotta for assistance with the SEM's and B. Stoeber, J. D. Olsen, and V.

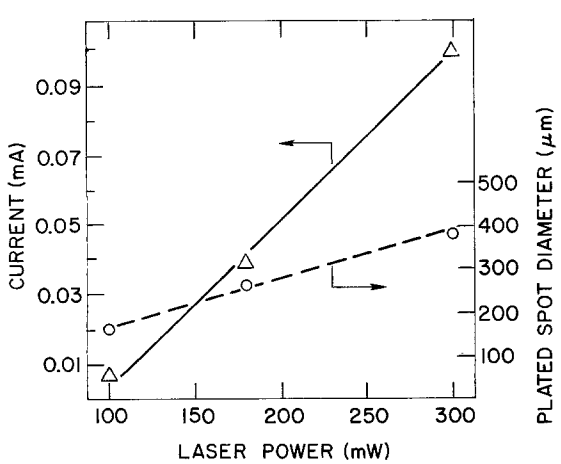

Fig. 16. Influence of the laser power on the deposition rate and deposited spot diameter. $Q = 5 \cdot 10^{-4}$C for each deposit; metallic film thickness, 10,000Å.

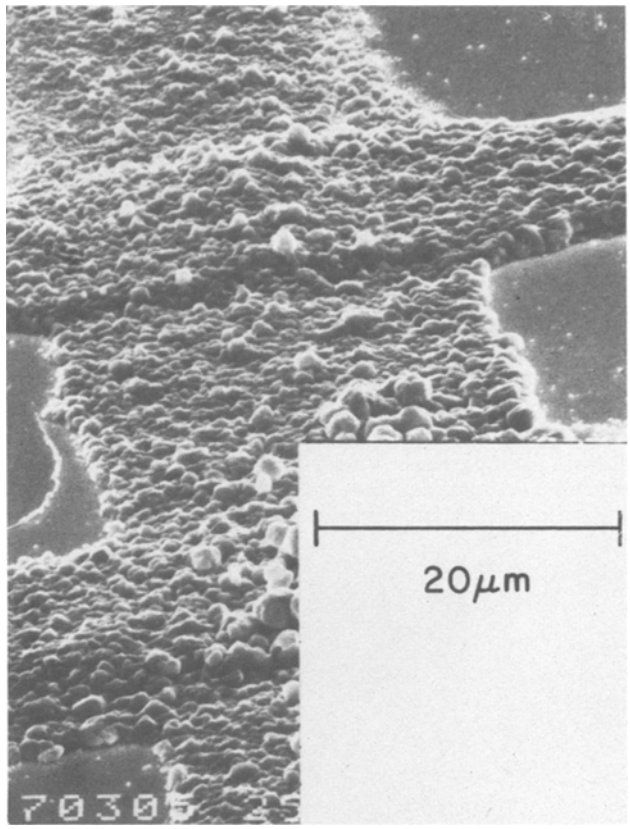

Fig. 17. SEM micrograph of a laser-enhanced plated bridge. Solution: $CuSO_4$, 0.5M; H_2SO_4, 0.01M. Laser power, 360 mW; laser light focused through a lens 20×; base: Nb, 200Å/Au, 1500Å with electroplated copper lines.

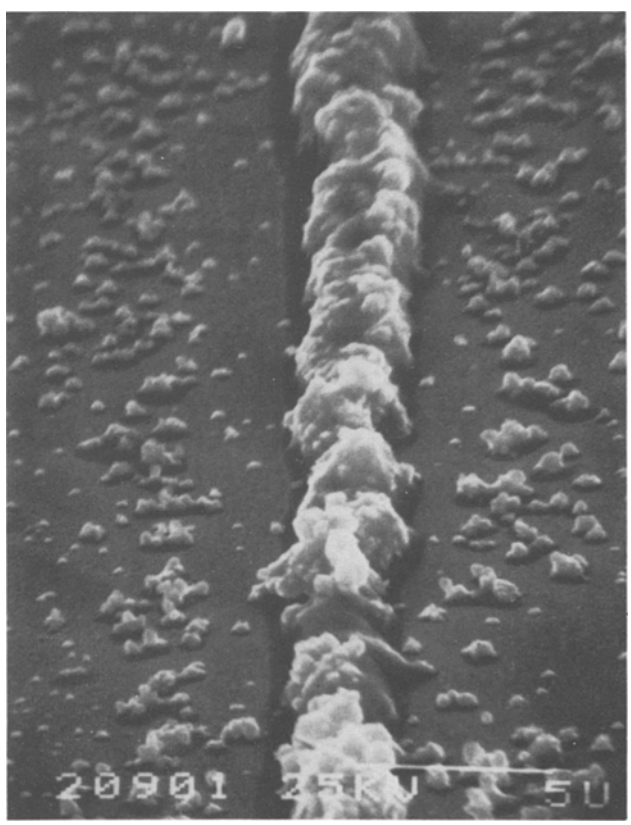

Fig. 18. Laser plated line of copper. Base: Nb, 200 Å/Cu, 1000Å evaporated on glass; laser beam focused through a microscope lens 20×; incident power, 50 mW.

Ranieri for technical contributions during various aspects of the research. We are also grateful to Dr. J. Cl. Chastang for his help in improving the optics of the experiment to obtain smaller plated deposits.

Manuscript received Feb. 24, 1981. This was Paper 373 presented at the Hollywood, Florida, Meeting of the Society, Oct. 5-10, 1980.

Any discussion of this paper will appear in a Discussion Section to be published in the June 1982 JOURNAL. All discussions for the June 1982 Discussion Section should be submitted by Feb. 1, 1982.

Publication costs of this article were assisted by IBM.

REFERENCES

1. R. J. von Gutfeld, E. E. Tynan, R. L. Melcher, and S. E. Blum, *Appl. Phys. Lett.*, **35**, 651 (1979).
2. R. J. von Gutfeld, E. E. Tynan, and L. T. Romankiw, Abstract No. 472, p. 1185, The Electrochemical Society Extended Abstracts, Los Angeles, CA (Oct. 14-19, 1979).
3. R. J. von Gutfeld and J. Cl. Puippe, *Oberfläche-Surface*, **11**, 294 (1981).
4. L. Kulynych, L. Romankiw, and R. J. von Gutfeld, *IBM Technical Disclosure Bulletin*, **23**, 1262 (1980).
5. K. J. Vetter, "Electrochemical Kinetics," p. 15, Academic Press, New York (1967).
6. J. Horkans, Unpublished results.

Ceramic-Coated Positive Current Collectors for Li-Al/LiCl-KCl/FeS_2 Batteries

G. Bandyopadhyay

Argonne National Laboratory, Materials Science Division, Argonne, Illinois 60439

ABSTRACT

Several electronically conducting ceramic and metallic coatings were investigated to determine their potential for use as current collectors in the positive electrodes of Li-Al/molten LiCl-KCl/FeS_2 battery cells. Static and in-cell corrosion tests in laboratory-scale cells were performed; the static tests were considerably more severe than the in-cell tests. Chemical vapor deposited (CVD) TiC and TiN coatings on inexpensive iron-based substrates showed significant promise in both tests. Analysis of the results led to the recommendation that the coating quality and thickness, the substrate type, the coating procedure, the design of the cell components, and the electrochemical conditions be optimized to achieve maximum coating stability in long-term operation of Li-Al/FeS_2 cells.

High performance Li-Al/iron sulfide secondary batteries are being developed by Argonne National Laboratory (ANL) (1) for electric vehicle propulsion and for energy storage in electric utility systems. In the cells of these batteries, negative electrodes of solid lithium-aluminum alloy and positive electrodes of iron sulfide (either FeS or FeS_2) are used. At an operating temperature of 400°-500°C, the electrolyte LiCl-KCl remains in a molten state (the eutectic melting point of the electrolyte is 352°C). The overall reaction that takes place in the Li-Al/FeS_x ($x = 1$ or 2) cell on discharge can be written as (2)

$$2x\text{Li-Al} + FeS_x \rightarrow x\text{Li}_2\text{S} + \text{Fe} + 2x\text{Al} \qquad [1]$$

where the composition of the positive electrode at complete discharge of a stoichiometric cell would be Li_2S and Fe. The reverse of these reactions occurs on recharging the cell.

Since the presence of lithium, lithium-aluminum, and iron sulfides makes the cell environment very reactive at elevated temperatures, the selection of suitable materials for various cell components is extremely critical for successful performance and commercialization of these batteries. The development of one such key component, the positive current collector, is the subject of this study.

Although low carbon or stainless steel performs reasonably well as the negative current collectors in Li-Al/FeS_x cells, extensive static, electrochemical, and in-cell corrosion testing of several commonly available metals and metallic alloys indicated that the selection of a suitable corrosion-resistant, cost-effective positive current collector poses a much more difficult problem (2-5). This is particularly true for FeS_2-type electrodes, in which the sulfur activity is considerably higher than that in FeS-type electrodes. Since Li-Al/FeS_2-type cells must be developed in order to achieve the long-term commercialization goals, it is important to identify and/or develop suitable positive current-collector materials for such cells. The only metal or metallic alloy that is known to exhibit the required chemical stability in an FeS_2-type electrode environment is molybdenum. However, molybdenum is expensive and difficult to fabricate in the shapes required for current-collector applications. Efforts are therefore underway to identify alternative positive current-collector materials for FeS_2-type cells. Electrically conducting ceramic coatings on inexpensive metallic substrates are being considered for such current-collector applications. The selection of suitable ceramics for coatings and the investigation of the stability of these coatings in static and in-cell corrosion environments is the subject of this paper.

Key words: corrosion, chemical vapor deposition, titanium nitride and titanium carbide coatings.

Selection of Materials

The criteria for the selection of ceramic coating materials for current-collector application include (*i*) sufficient electronic conductivity of the ceramic for adequate current-collection efficiency, (*ii*) corrosion resistance in the FeS_2 and LiCl-KCl environment at 400°-500°C, (*iii*) resistance to spalling under mechanical and thermal stresses, and (*iv*) cost effectiveness. Several metal borides, carbides, nitrides, and doped oxides are known to be good electronic conductors (6-8), and the coating technology of many of these materials is well developed (7, 9). Kuora *et al.* (10, 11) and Claar *et al.* (12) have performed preliminary